Ageing Assessment of XLPE LV Cables for Nuclear Applications Through Physico-Chemical and Electrical Measurements

SIMONE VINCENZO SURACI [1,2], **(Member, IEEE), DAVIDE FABIANI** [1], **(Senior Member, IEEE),**
ANNE XU [2], **SÉBASTIEN ROLAND** [2], **AND XAVIER COLIN** [2]

[1]LIMES – Department of Electrical, Electronic and Information Engineering "Guglielmo Marconi", University of Bologna, 40126 Bologna, Italy
[2]PIMM – Arts et Métiers Institute of Technology, 75013 Paris, France

Corresponding author: Simone Vincenzo Suraci (simone.suraci@unibo.it)

ABSTRACT This paper investigates the changes in electrical and physico-chemical properties of low-voltage power cables for nuclear application when subjected to the combined effects of gamma radiation and temperature. Electrical response is evaluated by means of the dielectric spectroscopy, while the physico-chemical changes are analyzed at different structural scales through five complementary techniques (OIT measurements, FTIR spectroscopy, swelling measurements, DSC analysis and micro-indentation). The dielectric spectroscopy and the first two chemical techniques are shown to be appropriate for evaluating the development of radio-thermal ageing in low-voltage cables. Hence, the results reported in this article suggest the effectiveness of dielectric spectroscopy as a non-destructive technique for on-site cable diagnosis.

INDEX TERMS Low-voltage cables, crosslinked polyethylene, gamma radiation, multiscale analysis, antioxidant migration, dielectric spectroscopy.

I. INTRODUCTION

Low-voltage (LV) cables are widely used in nuclear power plants (NPPs) for power transmission, control of equipment and instrumentation, communication (I&C) of signals and data. It has been estimated that there are about 1500 km of cables inside each NPP [1] and, since most of the NPPs built during the '80s and '90s are now reaching their end-of-life point, electric utility companies are trying to extend the NPPs operating life up to other 40 years. To reach this goal, assessing the health of LV I&C cables has become a key problem due to the fact that this is usually achieved through destructive techniques, e.g. mechanical tests [1, 2].
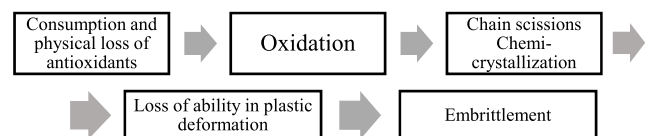
As known, the design of nuclear cables can differ depending on the applied voltage and specific application (control, power or instrumentation). In any case, the most sensitive part in terms of ageing is the electrical insulation which surrounds the conductor and whose extensive degradation can lead to the failure of the cable.

In extruded cables, electrical insulation is often made of polyethylene or ethylene-based copolymer formulated with different kinds of additives, above all antioxidants and flame

The associate editor coordinating the review of this manuscript and approving it for publication was Boxue Du.

retardants, which can reach very high concentrations (up to 2 wt% and 60 wt%, respectively) in LV cables. Antioxidants are needed to delay the onset of the polymer degradation and thus, to increase its lifetime [3]. However, in service, these additives can be consumed by specific chemical reactions [3], [4] and leave the insulation by migration, i.e. by diffusing through the insulating layer, then crossing its outer surface to reach the outside environment [5]–[7].

When the polymer matrix is no longer sufficiently protected, oxidation accelerates suddenly leading to the formation of a large variety of carbonyl and hydroxyl products [8], but also to consequential changes in the macro-molecular and morphological structures that are responsible for a catastrophic decay in fracture properties [9]. As an example, the following causal chain was established for linear PE [10]:

If the consequences of oxidation on the fracture properties of linear PE are now well understood and translated into

structure/property relationships [10], in contrast, a huge amount of work remains to be done concerning electrical properties.

The combined effects of ionizing radiation and temperature on PE insulation have been widely investigated from different perspectives and research fields. On one hand, the literature is plenty of studies on the characterization of the chemical degradation of this material, but without direct connection with its functional properties [11]–[15]. On the other hand, most electrical engineering studies have focused on the macroscopic behavior of this material for the application under consideration, not keeping into account the effects of damage and microstructural changes [16]–[18]. To date, too few studies have tried to establish relationships between the changes in electric properties and chemical composition of the insulation [19]–[25].

However, it is well known for a long time that some important electrical properties such as: dielectric constant and volume resistivity, are closely related to the chemical composition of the insulation [23], [26]. Both properties should change adversely when increasing the concentration of polar groups, e.g. carbonyl and hydroxyl products, during radio-thermal ageing. According to van Krevelen et al., the changes in dielectric constant could be predicted from a key chemical quantity (molar polarization) by using molar additivity rules, while the volume resistivity would be a decreasing exponential function of the dielectric constant [26]. In contrast, Darby et al. proposed a simple linear correlation between the dielectric constant and the solubility parameter (or cohesive energy density) [27]. But, a huge amount of work remains to be done to check the validity of these laws.

For this reason, in the cable industry, it is usual to select a fracture property to predict the insulation lifetime. In general, ultimate elongation is preferred because it varies monotonically with exposure time (contrarily to tensile strength) [28]. Thus, the conventional end-of-life criterion is 50% of the absolute value of the elongation-at-break [29]. However, in the context of an extension of the NPPs operating life, the use of a purely mechanical end-of-life criterion poses a serious problem in terms of cable life management. Indeed, in various technical works [2], [23], [30], it was observed that the elongation at break degrades faster than other functional properties of the cable (e.g. electrical). That is why, many research efforts are now undertaken to define a dielectric end-of-life criterion that would then be more realistic for LV cables used in NPPs.

This article aims at establishing the first correlations between the changes in chemical composition and electrical properties of the PE insulator during radio-thermal ageing. To reach this goal, a both multiscale and multidisciplinary approach was developed for analyzing all the structural changes susceptible to occur in the insulation. At the lowest scale (i.e. molecular), OIT measurements and FTIR spectroscopy were chosen to access the remaining concentration in antioxidants and detect the eventual traces of oxidation products, respectively. At the intermediary scales
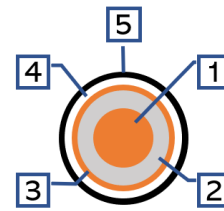

FIGURE 1. Multilayer structure of coaxial cables under investigation. (1) Conductor - Copper, (2) Primary insulation - XLPE, (3) Polymeric film - PET, (4) Shielding - Copper wire braid, (5) Sheath - Low smoke zero halogen.

(macromolecular and morphological), swelling measurements and DSC were used to detect chain scissions and monitor the changes in crystalline morphology, respectively. Finally, at the largest scale (macroscopic), dielectric spectroscopy and micro-indentation give access to the electrical and mechanical properties, respectively. At each scale, the changes with exposure time of relevant structural variables are determined and compared in order to establish the possible connections between these variables, i.e. structure/property relationships.

II. EXPERIMENTAL SETUP

A. SPECIMENS
The LV I&C cables under investigation are coaxial cables especially designed and produced for the European Project "TeaM Cables". Their multilayer structure is described in Fig. 1. These cables are made up of five concentric parts with the insulating layer being made of silane-crosslinked linear polyethylene (XLPE) stabilized with 1 phr of primary antioxidant (hindered phenol) and 1 phr of secondary antioxidant (thioether). Each cable specimen is about 50 cm long.

B. ACCELERATED AGING
Radio-thermal ageing was performed in the Panoza facility at UJV Rez, Czech Republic, with a ^{60}Co γ-ray source. The dose rate was set at 70 Gy/h for a temperature of 50 °C. Specimens were aged for 200 days and sampling was made about every 40 days. The maximum absorbed dose is 286 kGy.

C. ELECTRICAL MEASUREMENTS
Electrical properties, in particular the complex permittivity, were investigated by means of the dielectric spectroscopy with a Novocontrol Alpha Dielectric analyser. The complex permittivity $\dot{\varepsilon}$ is described as follows:

$$\dot{\varepsilon} = \varepsilon' - j\varepsilon''$$

where: ε' is the real part of permittivity defined as the dielectric constant of the material, and ε'' is the imaginary part of permittivity related to the dielectric losses of the material [1], [2], [19]–[25].

The instrumentation was set with the following test parameters:

- Applied voltage: 3 V_{rms};
- Frequency range: $10^{-2} - 10^{6}$Hz;
- Temperature: 50°C (in oven).

Input voltage was applied to the inner conductor through a BNC plug and output signal was obtained through the copper wire braid shielding.

The device requires, as an input, the reference capacitance in vacuum which was evaluated by reducing the cable geometry to a plane capacitor whose diameter D_{eq} was calculated through the following equation:

$$D_{eq} = \sqrt{\frac{8 \cdot d \cdot L}{\ln(R_2/R_1)}} \qquad (1)$$

where: d is the thickness of the insulation, L the length of the metallic mesh, and R_1 and R_2 the inner and outer radius of the electrical insulation, respectively.

Finally, the reference capacitance C_0 was calculated through:

$$C_o = \varepsilon_0 \frac{\pi \left(\frac{D_{eq}}{2}\right)^2}{d} \qquad (2)$$

where: ε_0 is the permittivity in vacuum.

D. PHYSICO-CHEMICAL CHARACTERIZATIONS

Before any physico-chemical analysis, the cables were stripped from their different successive layers using a specific cutting tool. All physico-chemical measurements were performed exclusively on the XLPE insulation.

1) OXIDATION INDUCTION TIME (OIT) MEASUREMENTS

DSC analysis was used to monitor the depletion in antioxidants in the insulation bulk during the radio-thermal ageing. Let us remember that OIT is the time required to induce the oxidation reaction of the polymer matrix under pure O_2 flow at high temperature (typically for T $\geq$ 190 °C). As the OIT of pure XLPE value is near zero at the temperatures under study, its measurement gives an assessment of the remaining antioxidant concentration in the aged insulation. Thus, when OIT vanishes, all antioxidants are chemically consumed.

OIT was measured at 210 °C with a TA instrument DSC Q10 calorimeter beforehand calibrated with an indium reference. Insulation samples with a mass ranged between 5 and 8 mg were introduced in an open standard aluminium pan to be submitted to the following program: first of all, heating from room temperature to 210 °C with an heating rate of 10 °C.min^{-1} under pure N_2 flow (50 mL.min^{-1}); then, temperature equilibration at 210 °C for 5 min; finally, switching the gas flow (50 mL.min^{-1}) from pure N_2 to O_2. The test was considered complete after the entire detection of an exothermal peak assigned to the oxidation reaction of XLPE. The OIT value was taken at the onset of the exothermal peak. This onset was determined graphically as the intersection point of the baseline with the steepest tangent of the increasing part of the exothermal peak (i.e. according to the so-called "tangent method").

2) FOURIER TRANSFORM INFRARED SPECTROSCOPY (FTIR)

FTIR spectroscopy was used to detect the changes in the chemical composition of the insulation during ageing (i.e. chemical consumption and migration of antioxidants, and XLPE oxidation). Insulation samples were analysed in the attenuated total reflectance (ATR) mode, both on their inner and outer surfaces and in the middle of their cross-section. FTIR spectra were recorded with a Perkin Elmer FTIR Frontier spectrometer equipped with a diamond/ZnSe crystal. Each spectrum corresponds to the average of 16 scans accumulation in the spectral range from 4000 to 650 cm^{-1}, with a resolution of 4 cm^{-1}. Any change in absorbance was normalized with the absorbance of CH_2 scissoring vibrations at 1472 cm^{-1} assigned to the PE crystal phase [31].

3) SWELLING MEASUREMENTS

Swelling and extraction in a good solvent were chosen to detect the consequences of XPLE oxidation on the structure of its macromolecular network (i.e. chain scissions versus crosslinking). Insulation samples with a mass ranged between 20 and 30 mg (m_i) were weighted with an accuracy of $\pm$ 0.01 mg and placed in a round-bottomed flask containing p-xylene (boiling point around 139 °C). This flask was connected to a water-cooled condenser and an adjustable heating mantle so that p-xylene could be heated to reflux. The samples were extracted in refluxing p-xylene for 24 h, then they were recovered from the solvent with the help of a funnel and filter paper. The excess solvent on the sample surface was carefully removed with the help of filter paper, then the samples were quickly transferred into a sealable pre-weighted sample vial and weighted to determine the mass of the swollen gel (m_{sw}). Final drying was carried out in a vacuum chamber at 80 °C up to reach the equilibrium mass of the dried gel (m_{gel}).

The gel content corresponding to the insoluble fraction (i.e. the proportion of chains participating to the macromolecular network) and swelling ratio can be expressed as follows:

$$\text{Gel content } (\%) = \frac{m_{gel}}{m_i} \times 100 \qquad (3)$$

$$\text{Swelling ratio } (\%) = \frac{m_{sw} - m_{gel}}{m_{gel}} \times 100 \qquad (4)$$

where m_i, m_{sw}, and m_{gel} are the respective masses of the initial sample, swollen gel, and dried gel.

4) DIFFERENTIAL SCANNING CALORIMETRY (DSC)

DSC analysis was chosen to detect the changes in crystalline morphology of XLPE during the radio-thermal ageing. Thermograms were recorded with a TA instrument DSC Q1000 calorimeter beforehand calibrated with an indium reference. Insulation samples with a mass ranged between 5 and 8 mg were introduced in a closed standard aluminium pan to be analysed between - 50 °C and 250 °C with heating and cooling rates of 10 °C.min^{-1} under pure N_2 flow of 50 mL.min^{-1}. The crystallinity ratio (χ_c) of the polymer

was determined as follows:

$$\chi_c = \frac{\Delta H_m}{\Delta H_{m,\infty}} \tag{5}$$

where ΔH_m and ΔH_∞ are the melting enthalpies (J.g^{-1}) of the sample and PE crystal, respectively. In literature, the commonly used value for ΔH_∞ is 290 J.g^{-1} [32], [33].

5) MICRO-INDENTATION
Micro-indentation was used to detect the consequences of the changes in macromolecular structure and crystalline morphology on the elastic properties of XLPE. As the material under study is the cable insulation, a prior flattening of the surface to be analysed is necessary. Thus, the insulation sample was embedded in a commercial acrylic KM-V resin in order to be polished with a series of abrasive papers of decreasing particle size (typically, from 80 to 2400 granulometry). Indentations were carried out on the outer surface of the insulation with a Micro-Indentation Tester from MSC Instrument equipped with a Vickers-type diamond tip of pyramidal geometry. The force applied was 150 mN, and the loading and unloading rates were 100 μm.min^{-1}. A pause of 30 s was systematically applied between the loading and unloading.

The indentation operating software gives directly the values of the reduced modulus (E_r) of the material and its Vickers hardness (HV), which are calculated according to the Oliver and Pharr's method [34], [35], as follows:

$$E_r = \frac{\sqrt{\pi S}}{2\beta\sqrt{A_c}} \tag{6}$$

$$HV = \frac{2F_{max}}{D^2} * \sin\alpha \tag{7}$$

where S is the initial slope of the unloading curve, β is a shape factor depending on the indenter type ($\beta = 1.012$ for a Vickers tip), and A_c is the contact area between the indenter and sample which is projected perpendicularly to the indenter axis on the sample surface. A_c is also directly given by the operating software and depends both on the penetration depth of the indenter and its geometry. α is the opening angle of the Indenter (68°), F_{max} the maximum applied force and D the measurement of the diagonal of the mark left by the indenter.

The Young's modulus (E) of the sample was then determined from the reduced modulus as follows:

$$E = \frac{1}{\frac{1-\vartheta^2}{E_r} - \frac{1-\vartheta_i^2}{E_i}} \tag{8}$$

where ϑ is the Poisson's coefficient of the sample ($\vartheta = 0.42$), and ϑ_i and E_i are respectively the Poisson's coefficient and Young's modulus of the diamond indenter ($\vartheta_i = 0.07$ and $E_i = 1147$ GPa).

6) OPTICAL MICROSCOPY
The results obtained with the previous analytical methods allowed building a possible ageing scenario for explaining the changes in electrical properties of the cable insulation. To check this scenario, a last complementary technique was
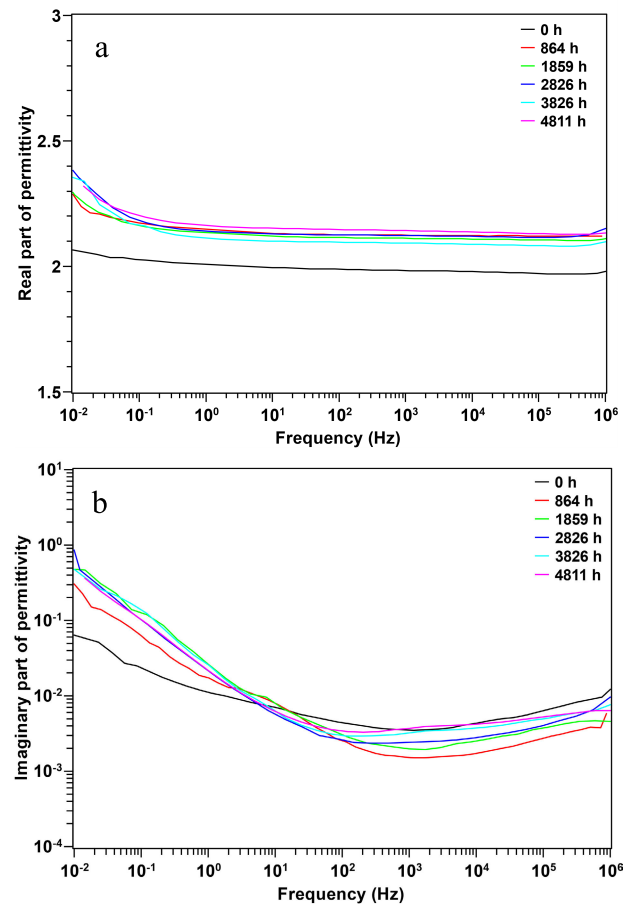

FIGURE 2. Dielectric spectra of the real (a) and imaginary (b) parts of permittivity for the analysed ageing periods.

used in this study. The outer surface of the insulating layer was examined with a Zeiss Axio Imager 2 optical microscope in reflection mode using a polarized light.

III. EXPERIMENTAL RESULTS
A. DIELECTRIC SPECTROSCOPY
Figure 2 shows the variation of the real (ε') and imaginary parts (ε'') of the permittivity as a function of frequency for the different ageing periods analysed here. As expected, both real and imaginary parts raise when increasing the ageing time.

Referring to Figure 2.a, the real part of the permittivity raises by a step of 0.2 during the first ageing period (51.2 kGy), then it remains almost constant in the further ageing periods. It is noteworthy that the trend of ε' is flat for most of the analysed frequency range, except for frequencies lower than 10^{-1} Hz where ε' raises while decreasing the applied frequency. This frequency dependence is presumably due to interfacial phenomena caused by ageing, as confirmed by the behaviour of ε'' (Figure 2.b). The imaginary part of permittivity shows an initial decrease in the first ageing period with respect to the unaged sample, while further ageing causes a quite linear increase of ε''. It is thus suspected that at least two physico-chemical mechanisms are in competition.
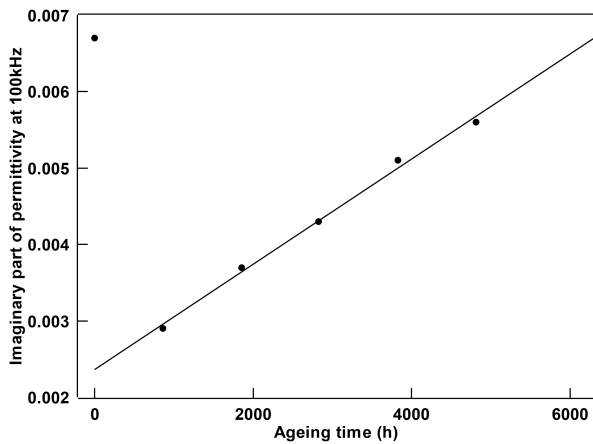
FIGURE 3. Imaginary part of the permittivity at 100 kHz as a function of ageing time.

Finally, focusing on the lowest frequency range (i.e. $10^{-2} - 10^1$ Hz), the value of the imaginary part of permittivity raises with decreasing the frequency. This behaviour is related to an important relaxation band occurring at lower frequencies (around 10^{-4} Hz) and linked to interfaces inside the tested cylindric capacitor, as it will be discussed in the following section.

Among the high frequencies, 100 kHz showed in literature [2], [19], [20], [23] to be representative of the dipolar response enhanced by ageing. Figure 3 shows the imaginary part of permittivity at 100 kHz plotted as a function of the total absorbed dose.

B. OIT MEASUREMENTS

Figure 4 displays the OIT thermograms of the insulating layer after different irradiation doses (a) and the corresponding changes in OIT with ageing time (b). It can be observed that OIT decreases during the radio-thermal ageing, which is presumably due to the chemical consumption of antioxidants by specific chemical reactions and/or their migration from the bulk to the insulation surface. The drop in OIT is particularly drastic during the first ageing period (corresponding to a total irradiation dose of 51.2 kGy), for which OIT is reduced by a factor of about 6. Then, OIT is still decreasing but more slowly. Finally, it reaches a very low but non-null value (typically 2 minutes) for the highest irradiation dose under study. At 286 kGy, oxidation of XLPE has not started yet.

C. FTIR SPECTROSCOPY

Figure 5 shows the main changes in the FTIR spectrum of the outer surface of the insulating layer. These changes occur in three specific spectral regions: (a) between 3500 and 3800 cm^{-1} (hydroxyls), (b) 1600 and 1850 cm^{-1} (carbonyls), and (c) between 900 and 1500 cm^{-1}.

In the carbonyl region (Figure 5.b), a single IR absorption band was initially observed at 1737 cm^{-1} for the unaged material, attributed to the ester groups of both phenol and thioether antioxidants. Then, two new bands appear in this
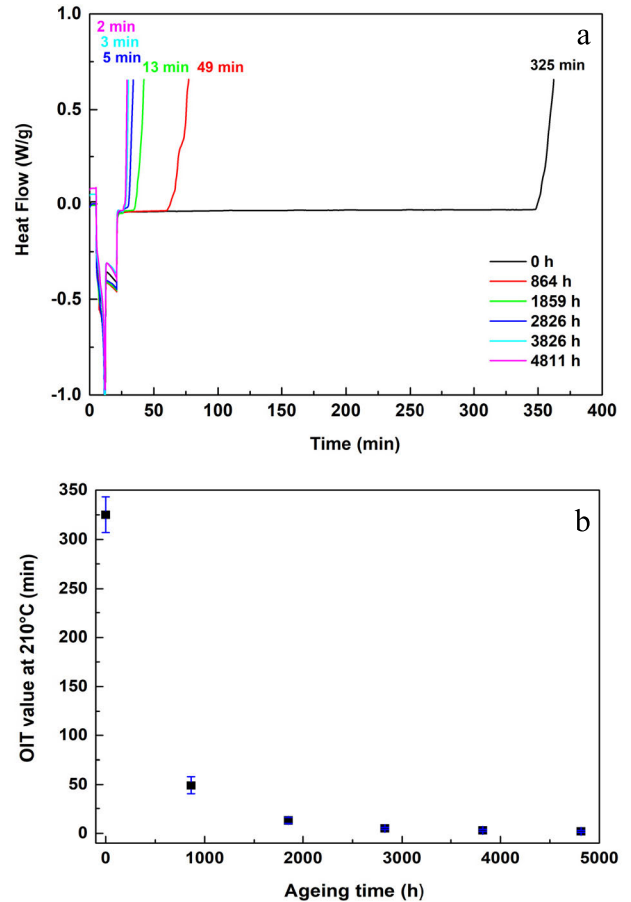

FIGURE 4. (a) OIT thermograms at 210 °C after different irradiation doses. (b) Corresponding changes in OIT with ageing time.

spectral region for the aged material: a shoulder at 1720 cm^{-1} and another main band at 1742 cm^{-1}. These latter two peaks increase with exposure time on the insulation surface.

Similarly, in the hydroxyl region (Figure 5.a), a single and small IR absorption band was observed at 3640 cm^{-1} for the unaged material. This band was assigned to the phenol function of the phenolic antioxidant. This band disappears on the insulation surface while two new small bands, around 3609 and 3580 cm^{-1}, appear and increase, then decrease with exposure time.

Finally, in the region between 900 and 1500 cm^{-1} (Figure 5.c), the IR absorption bands at 1366, 1262, 1238, 1186, and 1085 cm^{-1} initially observed for the unaged sample are probably due to the C-O bonds of the ester groups of both antioxidants. Like the carbonyl bands, these latter increase with exposure time. Other IR absorption bands appear at 1028, 1046, 1131, and 1313 cm^{-1} on the insulation surface, which could be assigned to the oxidation products of thioether antioxidant (in particular, sulfoxide and sulfone species) formed during the stabilization reactions involving this antioxidant.

Figure 6 shows the changes in the FTIR spectrum obtained in the bulk of the insulating layer (exclusively in the carbonyls region). The same observations can be made as previously
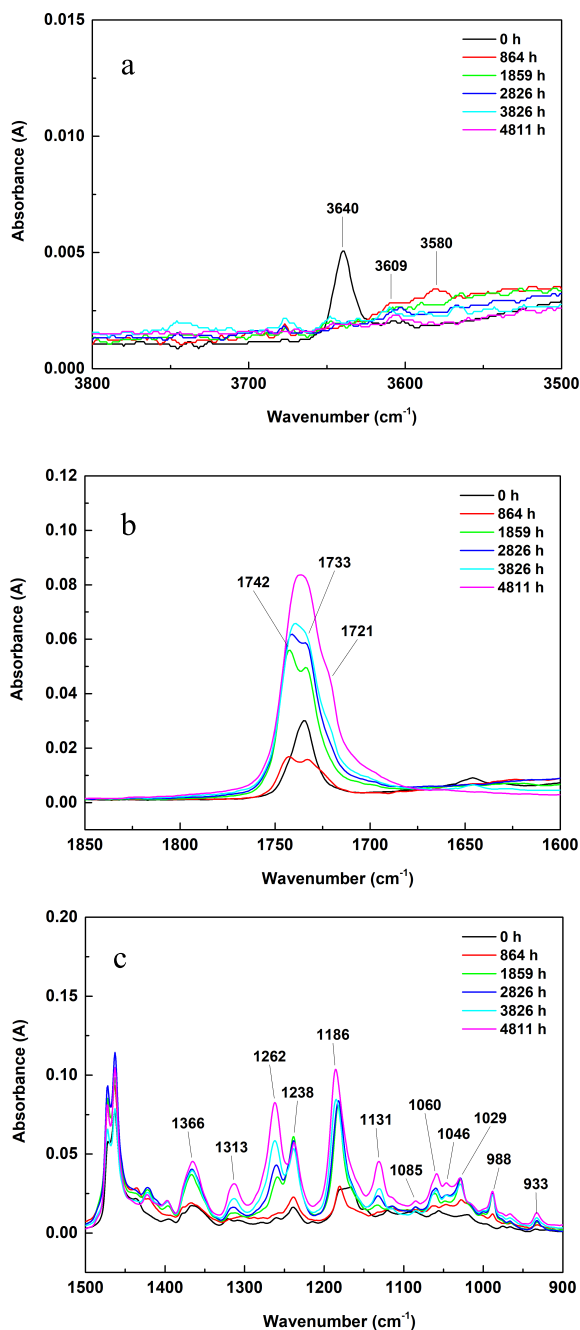
FIGURE 5. FTIR spectra of the outer surface of the insulating layer (a) between 3500 and 3800 cm-1, (b) 1600 and 1850 cm-1 and (c) 900 and 1500 cm-1.

reported, referring to the presence of a single IR absorption band at 1737 cm^{-1} for the unaged sample. Then, this band seems to slightly decrease during the first ageing duration to finally remain almost constant with eventually the appearance of a small shoulder at 1720 cm^{-1} during the last ageing durations.

Figure 7 reports the changes in ester index (i.e. absorbance ratio between the sum of all ester bands and the reference band at 1472 cm^{-1}) with exposure time in the bulk and on the outer surface of the insulation. The ester index quickly
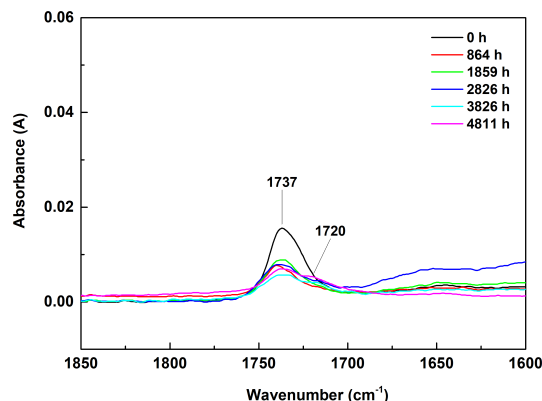

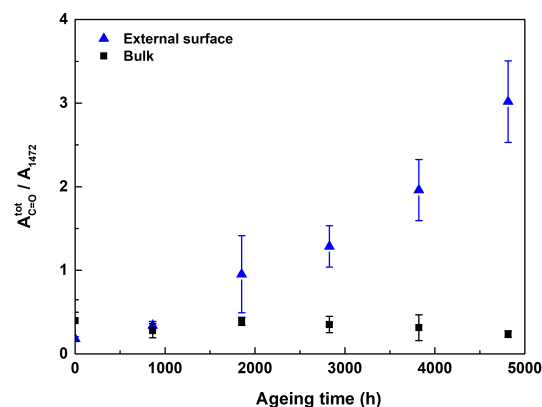**FIGURE 6.** FTIR spectra obtained in the bulk of the insulating layer between 1600 and 1850 cm-1.

FIGURE 7. Changes in ester index with ageing time in the bulk and on the outer surface of the insulating layer.

increases with ageing time on the outer surface, especially from the second ageing duration, while it slowly decreases in the bulk.

D. SWELLING AND GEL RATIO
In Figure 8, the changes in gel content (a) and swelling ratio (b) of the insulating layer are displayed as a function of exposure time. No significant change in gel content is observed during the radio-thermal ageing. Concerning swelling ratio, however, a small increase is observed between the second and third irradiation dose, after which it remains almost constant. If merging both results, it can be concluded that a very small number of chain scissions have occurred, but they have not led to the formation of linear macromolecular fragments yet, but only to the formation of dangling chains. This is a typical behavior for very low oxidation ratios, often undetected by conventional spectrochemical methods (such as FTIR) due to their poor sensitivity threshold.

E. DSC ANALYSIS
Figure 9 reports the DSC thermograms of the insulating layer after different irradiation doses (a) and the corresponding changes in cristallinity ratio with ageing time (b). No significant change in cristallinity and melting temperature are
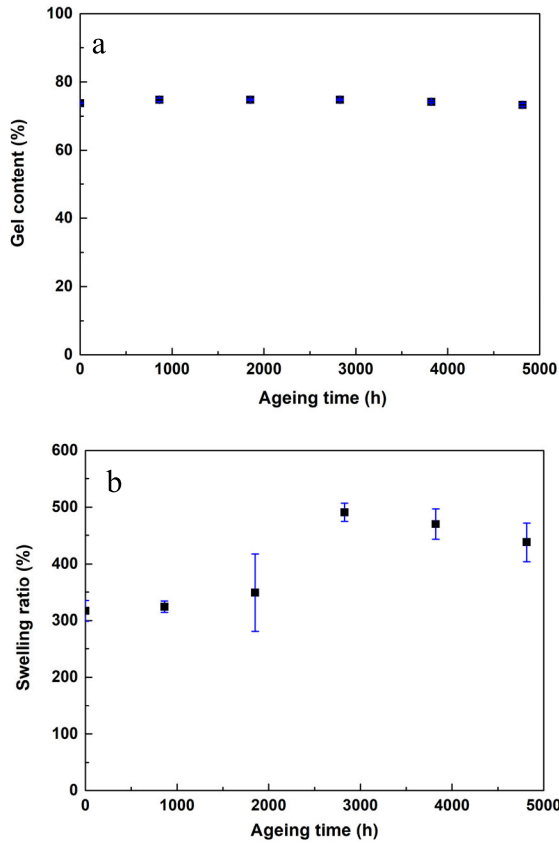
FIGURE 8. (a) Changes in the gel content and (b) swelling ratio with ageing time.

FIGURE 9. (a) DSC thermograms after different irradiation doses. (b) Changes in cristallinity ratio with ageing time.

observed during the radio-thermal ageing. This result confirms the absence of short macromolecular fragments in the aged material, otherwise these latter would have migrated up to the surface of the pre-existing crystals to thicken them (chemi-crystallization) [10].

F. MICRO-INDENTATION MEASUREMENT

Figure 10 shows the changes in Young's modulus on the outer surface of the insulation with ageing time. As for swelling ratio, a small decrease in the Young's modulus is observed between the second and third irradiation dose, after which it remains almost constant. This small decrease is presumably due to a small number of chain scissions. Indeed, it is well known that the Young's modulus (E) of an elastomer is related to the concentration of chains participating to the macromolecular network (ν), more commonly called the elastically active chains, through the Flory's theory [36]:

$$E = 3\nu\rho RT \tag{9}$$

where ρ the volumic mass of XLPE, R the universal gas constant and T the temperature (expressed in K).

Hence, when chain scissions predominate over crosslinking, the concentration of elastically active chains decreases, then causing the decrease of the Young's modulus.
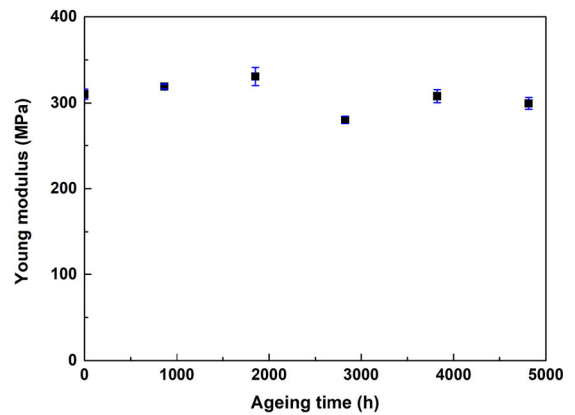

FIGURE 10. Changes in Young's modulus on the outer surface of the insulation with ageing time.

G. OPTICAL MICROSCOPY

Among all the physico-chemical mechanisms put in evidence in the previous sections, the migration of antioxidants from the bulk to the insulation surface appear to predominate the most largely. A complementary technique used to confirm this assumption is optical microscopy.

The insulation surface was examined by optical microscopy in reflection mode before and after radio-thermal
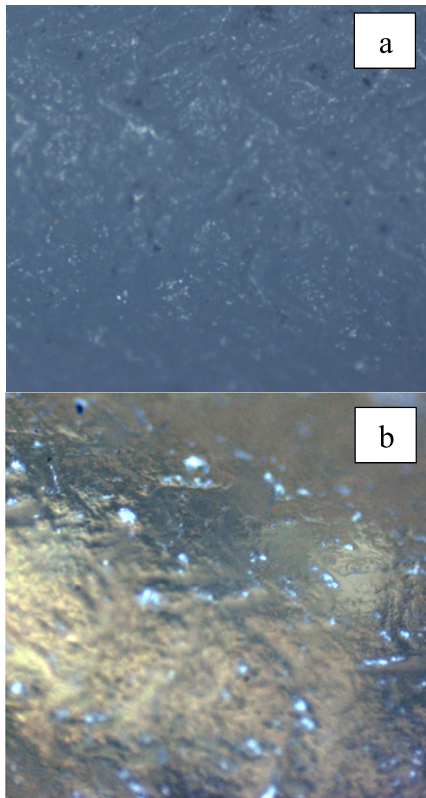
FIGURE 11. Micrographs of the outer surface of the insulation: before (a) and after 4811 hours (b) of radio-thermal ageing. Magnification is 50x.

ageing. Initially, this surface is relatively flat and homogeneous but during ageing it becomes rougher and yellowish, as expected (see Figure 11). Indeed, a huge quantity of polyhedral crystals, due to the exudation of antioxidants from the insulation, are formed on the insulation surface. These crystals are clearly observed in the form of bright dots after 4800 hours of radio-thermal ageing (Figure 11b).

Such an exudation process was already evidenced during the thermal treatment at moderate temperature (typically 70°C) of model XLPE samples stabilized with a phenol antioxidant [7]. As shown by these authors, the reorganization of antioxidant molecules in different forms (dissociated or crystalline structures) results in the appearance of new IR absorption bands of antioxidants. However, in this study, the presence of two different types of antioxidants (phenol and thioether) absorbing in the same ranges of wavenumbers, seriously complicates the analysis of experimental results and thus, does not allow the attributions of the IR bands observed in Figures 5 and 6.

IV. DISCUSSION

The frequency range investigated through dielectric spectroscopy is referred to both lower frequencies dipolar polarization ($10^6 - 10^2$ Hz) and interfacial polarization (lower than 10^2 Hz). This latter is usually known as Maxwell-Wagner-Sillars polarization [37] and it is caused by the limited diffusion of space charges inside the dielectric by means of the

applied electric field. These charges may settle next to interfaces or discontinuities inside the dielectric itself. As known, interfaces can be at least of two different types:

  i. Chemical interfaces between two materials of different chemical composition, for instance in a multilayer structure (inter-layers interface) and in composite materials (fiber/matrix interface);

 ii. Physical interfaces between materials of the same chemical composition but of different physical state, for instance in semi-crystalline polymers (amorphous/crystal interface).

From the multilayer structure of the coaxial cable sample described in Figure 1, a polymeric film is placed between the primary insulation (XLPE) and the external copper braid, in order to protect the primary insulation during the processing operations. Due to the experimental setup used, analyses include this film whose interface between the copper braid and the insulation is prone to charge accumulation. This gives rise to the polarization peak discussed in the previous section, which also appear for the whole set of specimens considered (both unaged and aged samples). Furthermore, this peak increases with ageing, suggesting that this latter leads to the creation of new interfaces during the radio-thermal ageing inside the primary insulation. This interface polarization may be related to the conductive AO layer abovementioned, rather than the presence of ionic and radical species created during the ageing process, which can migrate because of the electric field applied and may collect near the interfaces.

Moreover, FTIR also highlighted the migration of antioxidants from the bulk to the insulation surface with the appearance of new absorption bands of ester (at 1720 and 1742 cm^{-1}) and phenol functions (at 3580 and 3609 cm^{-1}) (see Figure 5). These new bands could be assigned to different crystalline structures of antioxidants formed on the insulation surface. This phenomenon called polymorphism have already been observed in literature for several phenol antioxidants [7], [38].

Otherwise, the highest frequency range analysed, as reported in literature [19], [20], [23], [24] and previously discussed, is related to the polarization of large dipolar species. These ones, e.g. oxidized polymer groups, are often created through the action of ageing factors like e.g. high temperatures and radiation, which catalyse oxidative reactions mainly responsible for the degradation of polymers [1], [19], [20], [23], [24]. For this reason, the high frequency range of the imaginary part of permittivity has been shown in previous works [1], [19], [20], [23], [24] to be associated with the growth of oxidative products in the polymer matrix during ageing.

Nevertheless, it is worth commenting that, for cables here investigated, ageing conditions do not yield to a significant oxidation of the primary insulation as shown by the physicochemical analysis. Indeed, as it can be seen in Figure 4, OIT decreases with ageing but still remains non-null, meaning that antioxidants are still present and protect the cable insulation against oxidation. Gel content and crystallinity ratio also do

not display significant variation during ageing (see Figure 8a and Figure 9b), meaning that very small changes in the macromolecular network of XLPE have occurred.

The drastic decrease of the imaginary part of permittivity observed during the first ageing period (Figure 2b) could be due to the chemical consumption of antioxidants. Indeed, OIT decreases drastically during this first period (Figure 4) while the active functions of phenolic antioxidants disappear (at $3640\,\mathrm{cm}^{-1}$) and those of thioester antioxidants are converted into sulfoxide and sulfone functions (at 1028, 1046, 1131 and $1313\,\mathrm{cm}^{-1}$) (see Figure 5).

The accumulation of antioxidants during ageing on the outer surface of the insulation could create a thin layer exhibiting a higher electrical conductivity than the primary insulation, which can give rise to the high frequency electrical response. Indeed, the AOs molecules, which accumulates in the layer on the outer insulation surface, can act as induced dipoles following the applied alternating electric field even at high frequencies, similarly to ionic polarization which may occur in crystals causing the raise of dielectric losses in the high frequency region (Figure 2b). Moreover, the longer is the ageing period, the higher is the increase of AOs molecules on the outer surface (as reported in Figure 7). The accumulation of these highly dipolar species may affect the highest frequency range dielectric response, raising the value of ε'' as reported in Figure 2b.

As a result, the antioxidant migration and accumulation on the insulation surface could be the cause of a dielectric response increase shown in Figure 2b for doses higher than 51 kGy, as well as the formation of dipolar products created by ageing which enhance the electric response in the high frequency region [19], [20], [23], [24].

As presented in Figure 3, the value of ε'' shows an abrupt reduction imputable to the huge antioxidants consumption as confirmed by the OIT measurements (Figure 4b). The regression line showed in Figure 3 (built from the first ageing period) well fits with the total dose absorbed by the specimens during ageing. This behaviour confirms the strict correlation between evolution of ageing and, contextually, its products (above all dipolar species), and the imaginary part of permittivity at 10^5 Hz. Therefore, ε'' at 100 kHz may be also used as an indicator for development of dielectric properties of the material with ageing other than a marker for ageing state of the insulation.

V. CONCLUSIONS

This paper investigated the changes during radio-thermal ageing of the electrical and physical-chemical properties of LV XLPE insulated cables for NPPs application. Cable ageing has been monitored through six different analytical techniques, allowing a spread characterization of the analysed XLPE insulation. In particular, the changes in physical-chemical properties has been correlated to the increase of ε'', and contextually, to the dielectric losses in the highest frequency range.

It has been shown that radio-thermal ageing caused an important chemical consumption of antioxidants (showed by OIT measurements) leading to an abrupt decrease of the imaginary part of permittivity (Figure 2b) during the first ageing period. Further ageing has caused the migration of antioxidants from the bulk to the insulation surface (as shown by the increase of the ester index in Figure 7). These molecules, as highly conductive, caused the raise of the imaginary part of permittivity with exposure time.

In conclusion, it has been shown that the imaginary part of permittivity and, in general, the dielectric losses, can be related to the formation of a thin conductive layer of antioxidant crystals on the insulation surface during radio-thermal ageing.

Further research will include the changes in mechanical properties (e.g. elongation-at-break) and other electrical properties (e.g. conductivity) in order to obtain a complete view of the consequences of radio-thermal ageing from the lowest (i.e. molecular) to largest (i.e. macroscopic) scale.

REFERENCES

[1] *Management of Life Cycle and Ageing at Nuclear Power Plants: Improved I&C Maintenance*, Int. At. Energy Agency, Vienna, Austria, 2004.

[2] L. Verardi, "Aging of nuclear power plant cables: In search of non-destructive diagnostic quantities," Ph.D. dissertation, Dept. Elect., Electron. Inf. Eng., Guglielmo Marconi, Univ. Bologna, Italy, 2014.

[3] H. Zweifel and S. E. Amos, *Plastics Additives Handbook*, 5th ed. Munich, Germany: Hanser, 2001.

[4] W. L. Hawkins, *Polymer Stabilization*. New York, NY, USA: Wiley, 1971.

[5] N. C. Billingham and P. D. Calvert, "The physical chemistry of oxidation and stabilisation of polyolefins," in *Developments in Polymer Stabilization*, vol. 3, G. Scott, Ed. London, U.K.: Applied Science, 1980, p. 139.

[6] J. Y. Moisan, "Diffusion des additifs du polyethylene—I: Influence de la nature du diffusant," *Eur. Polym. J.*, vol. 16, no. 10, pp. 979–987, 1980.

[7] A. Xu, S. Roland, and X. Colin, "Physico-chemical characterization of the blooming of Irganox 1076 antioxidant onto the surface of a silane-crosslinked polyethylene," *Polym. Degradation Stability*, vol. 171, Jan. 2020, Art. no. 109046.

[8] M. Da Cruz, L. Van Schoors, K. Benzarti, and X. Colin, "Thermo-oxidative degradation of additive free polyethylene. Part I. Analysis of chemical modifications at molecular and macromolecular scaless," *J. Appl. Polym. Sci.*, vol. 133, no. 18, May 2016, Art. no. 43287.

[9] A. F. Reano, A. Guinault, E. Richaud, and B. Fayolle, "Polyethylene loss of ductility during oxidation: Effect of initial molar mass distribution," *Polym. Degradation Stability* vol. 149, pp. 78–84, Mar. 2018.

[10] B. Fayolle, E. Richaud, X. Colin, and J. Verdu, "Review: Degradation-induced embrittlement in semi-crystalline polymers having their amorphous phase in rubbery state," *J. Mater. Sci.*, vol. 43, no. 22, pp. 6999–7012, Nov. 2008.

[11] V. Langlois, M. Meyer, L. Audouin, and J. Verdu, "Physical aspects of the thermal oxidation of crosslinked polyethylene," *Polym. Degradation Stability*, vol. 36, no. 3, pp. 207–216 1992.

[12] V. Langlois, L. Audouin, J. Verdu, and P. Courtois, "Thermooxidative aging of crosslinked linear polyethylene: Stabilizer consumption and lifetime prediction," *Polym. Degradation Stability*, vol. 40, no. 3, pp. 399–409, 1993.

[13] N. Khelidj, X. Colin, L. Audouin, J. Verdu, C. Monchy-Leroy, and V. Prunier, "Oxidation of polyethylene under irradiation at low temperature and low dose rate. Part I. The case of 'pure' radiochemical initiation," *Polym. Degradation Stability*, vol. 91, no. 7, pp. 1593–1597, 2006.

[14] N. Khelidj, X. Colin, L. Audouin, J. Verdu, C. Monchy-Leroy, and V. Prunier, "Oxidation of polyethylene under irradiation at low temperature and low dose rate. Part II. Low temperature thermal oxidation, *Polym. Degradation Stability*, vol. 91, no. 7, pp. 1598–1605, Jul. 2006.

[15] X. Colin, C. Monchy-Leroy, L. Audouin, and J. Verdu, "Lifetime prediction of polyethylene in nuclear plants," *Nucl. Instrum. Methods Phys. Res. B, Beam Interact. Mater. At.*, vol. 265, no. 1, pp. 251–255, Dec. 2007.

[16] N. Bowler and S. Liu, "Aging mechanisms and monitoring of cable polymers," *Int. J. Prognostics Health Manage.*, vol. 6, pp. 1–12, 2015.

[17] T. Han, B. Du, J. Su, Y. Gao, Y. Xing, S. Fang, C. Li, and Z. Lei, "Inhibition effect of graphene nanoplatelets on electrical degradation in silicone Rubber," *Polymers*, vol. 11, no. 6, p. 968, Jun. 2019, doi: 10.3390/polym11060968.

[18] Y. Wang, A. Zhao, X. Zhang, Y. Shen, F. Yang, J. Deng, and G. Zhang, "Study of dielectric response characteristics for thermal aging of XLPE cable insulation," in *Proc. Int. Conf. Condition Monitor. Diagnosis (CMD)*, Xi'an, China, Sep. 2016, pp. 602–605.

[19] E. Linde, L. Verardi, D. Fabiani, and U. Gedde, "Dielectric spectroscopy as a condition monitoring technique for cable insulation based on crosslinked polyethylene," *Polym. Test.*, vol. 44, pp. 135–142, Jul. 2015.

[20] E. Linde, L. Verardi, P. Pourmand, D. Fabiani, and U. Gedde, "Nondestructive condition monitoring of aged ethylene-propylene copolymer cable insulation samples using dielectric spectroscopy and NMR spectroscopy," *Polym. Test.*, vol. 46, pp. 72–78, Sep. 2015.

[21] A. Sriraman, N. Bowler, S. Glass, and L. S. Fifield, "Dielectric and mechanical behavior of thermally aged EPR/CPE cable materials," in *Proc. IEEE Conf. Electr. Insul. Dielectric Phenomena (CEIDP)*, Oct. 2018, pp. 598–601.

[22] T. Salivon, X. Colin, and R. Comte, "Degradation of XLPE and PVC cable insulators," in *Proc. IEEE Conf. Electr. Insul. Dielectric Phenomena (CEIDP)*, Oct. 2015, pp. 656–659.

[23] S. V. Suraci, D. Fabiani, H. Joki, and K. Sipilä, "Filler impact analysis on aging of crosslinked polyethylene for nuclear applications through dielectric spectroscopy," in *Proc. IEEE Conf. Elect. Insul. Dielectric Phenomena (CEIDP)*, 2019, pp. 175–178.

[24] S. V. Suraci, D. Fabiani, L. Mazzocchetti, V. Maceratesi, and S. Merighi, "Investigation on thermal degradation phenomena on low density polyethylene (LDPE) through dielectric spectroscopy," in *Proc. IEEE Conf. Electr. Insul. Dielectric Phenomena (CEIDP)*, Oct. 2018, pp. 434–437.

[25] I. L. Hosier, J. E. A. Koilraj, and A. S. Vaughan, "Effect of aging on the physical, chemical and dielectric properties of dodecylbenzene cable oil," in *Proc. IEEE Int. Conf. Dielectr. (ICD)*, vol. 2, Jul. 2016, pp. 812–815.

[26] D. W. Van Krevelen and K. Te Nijenhuis, *Properties of Polymers. Their Estimation and Correlation With Chemical Structure. Their Numerical Estimation and Prediction From Additive Group Contributions*, 4th ed. Amsterdam, The Netherlands: Elsevier, 2009, ch. 11, p. 319.

[27] J. R. Darby, N. W. Touchette, and K. Sears, "Dielectric constants of plasticizers as predictors of compatibility with polyvinyl chloride," *Polym. Eng. Sci.*, vol. 7, no. 4, pp. 295–309, Oct. 1967.

[28] B. Fayolle, L. Audouin, and J. Verdu, "Oxidation induced embrittlement in polypropylene—A tensile testing study," *Polym. Degradation Stability*, vol. 70, no. 3, pp. 333–340, Jan. 2000.

[29] N. Khelidj, X. Colin, L. Audouin, and J. Verdu, "A simplified approach for the lifetime prediction of PE in nuclear environments," *Nucl. Instrum. Methods Phys. Res. B, Beam Interact. Mater. At.*, vol. 236, nos. 1–4, pp. 88–94, Jul. 2005.

[30] *Initial Acceptance Criteria Concepts and Data for Assessing Longevity of Low-Voltage Cable Insulations and Jackets*, Electr. Power Res. Inst., Palo Alto, CA, USA, 2005.

[31] P. Pagès. (2005). *Characterization of Polymer Materials Using FT-IR and DSC Techniques, Universidade da Coruña*. Accessed: Apr. 25, 2019. [Online]. Available: http://ruc.udc.es/dspace/handle/2183/11499

[32] S. Bensason, J. Minick, A. Moet, S. Chum, A. Hiltner, and E. Baer, "Classification of homogeneous ethylene-octene copolymers based on comonomer content," *J. Polym. Sci. B, Polym. Phys.*, vol. 34, no. 7, pp. 1301–1315, May 1996.

[33] K. Sirisinha and S. Chimdist, "Comparison of techniques for determining crosslinking in silane-water crosslinked materials," *Polym. Test.*, vol. 25, no. 4, pp. 518–526, Jun. 2006.

[34] T. Iqbal, B. Briscoe, and P. Luckham, "Surface plasticization of poly(ether ether ketone)," *Eur. Polymer J.*, vol. 47, no. 12, pp. 2244–2258, Dec. 2011.

[35] E. Courvoisier, Y. Bicaba, and X. Colin, "Multi-scale and multi-technical analysis of the thermal degradation of poly(ether imide)," *Polym. Degradation Stability*, vol. 147, pp. 177–186, Jan. 2018.

[36] P. J. Flory, *Principles of Polymer Chemistry*. Ithaca, NY, USA: Cornell Univ. Press, 1953.

[37] S. V. Suraci, D. Fabiani, and C. Li, "Additives effect on dielectric spectra of crosslinked polyethylene (XLPE) used in nuclear power plants," in *Proc. IEEE Elect. Insul. Conf. (EIC)*, 2019, pp. 410–413.

[38] J. Saunier, V. Mazel, C. Paris, and N. Yagoubi, "Polymorphism of Irganox 1076: Discovery of new forms and direct characterization of the polymorphs on a medical device by Raman microspectroscopy," *Eur. J. Pharmaceutics Biopharmaceutics*, vol. 75, no. 3, pp. 443–450, Aug. 2010.

SIMONE VINCENZO SURACI (Member, IEEE) was born in Reggio Calabria, Italy, in 1993. He received the B.Sc. degree in civil and environmental engineering from the University of Reggio Calabria, in 2015, and the M.Sc. degree in energy and nuclear engineering from the University of Bologna, in 2017. He is currently pursuing the Ph.D. degree in electrical engineering and polymer sciences with the University of Bologna and at the Arts et Métiers Institute of Technology, Paris.

His research interests include the study of polymeric dielectrics for nuclear applications and their degradation with aging, nondestructive diagnosis techniques for insulation materials, and nano-structured composites. He has been member of DEIS, since 2017.

DAVIDE FABIANI (Senior Member, IEEE) received the M.Sc. and Ph.D. degrees (Hons.) in electrical engineering in 1997 and 2002, respectively. He is currently an Associate Professor with the Department of Electrical Electronics and Information Engineering, University of Bologna. His fields of research are mainly related to development, characterization, and diagnosis of electrical insulation systems for applications in electrical and electronic apparatus. He is the author or coauthor of about 180 articles, most of them published on the major international journals and conference proceedings. He is an Associate Editor of the IEEE TRANSACTIONS ON DIELECTRICS AND ELECTRICAL INSULATION and *IET High Voltage Journal*. He is currently a member of DEIS AdCom and the Chair of the Meetings Committee, since 2016.

ANNE XU received the B.S. degree in chemistry from the University Pierre et Marie Curie, Paris, France, in 2014, and the M.S. degree in chemical science and engineering from Chimie ParisTech, Paris, in 2017. She is currently pursuing the Ph.D. degree in polymer sciences with the PIMM Laboratory, Arts et Métiers Institute of Technology, Paris.

In 2016, she was an Industrial Trainee at the CSIRO's Material Sciences and Engineering Division, Clayton, VIC, Australia. In 2017, she was a Research Intern at the LICSEN Laboratory, CEA, Saclay, France. She is the coauthor of one peer-reviewed publication. Her research interests include the synthesis and the establishment of structure-properties relationships of polymeric materials, and the study of their durability and stabilization under different environmental stresses.

SÉBASTIEN ROLAND was born in Saint-Germain-en-Laye, France, in 1983. He received the M.Sc. degree in chemistry from the École Nationale Supérieure de Physique-Chimie (ENSCPB), Bordeaux, in 2006, and the Ph.D. degree in polymer science from the University of Montréal, Canada, in 2013.

From 2013 to 2015, he worked as a Postdoctoral Fellow and then as a Research and Teaching Assistant with the PIMM Laboratory, Arts et Métiers Institute of Technology (ENSAM), Paris, France, where he has been an Assistant Professor, since 2015. He is the coauthor of 16 peer-reviewed articles. His research activities focus on the structure-properties relationships of polymeric materials in the bulk as well as in thin films.

XAVIER COLIN has been a Professor at ENSAM (Arts et Métiers Institute of Technology), Paris, France since September 2011. He prepared a Ph.D. thesis in ONERA, Châtillon, France in collaboration with EADS, Suresnes, France on the thermal oxidation of organic composite materials considered as warm structural parts for the next generation supersonic aircraft. He defended this Ph.D. thesis in 2000 in the specialty ''Mechanics and Materials'' at ENSAM, Paris, France, and he obtained the highest honors distinction with the jury's congratulations.

After a Postdoctoral Internship with CEA, Grenoble, France, he joined the team of Prof. J. Verdu at ENSAM, Paris, as a Research Engineer, then as a Professor Assistant, in 2002. He received the HDR thesis (required for a full professor position in France) in chemistry on the theme: Towards a model for predicting the lifetime of polymer structures in their use conditions at UPMC, Paris, in 2008. Since September 2011, he has been a Professor at ENSAM. He is the author of one book and 17 chapters in edited books. He has authored more than 90 articles in refereed journals, and more than 220 communications in conferences, including 43 invited lectures. His research interests include ageing and durability of polymers and organic composite materials, multiscale and multitechniques analysis of physical and chemical ageing processes, as well as their consequences on functional properties; kinetic analysis and modeling, development of structure/property relationships, and proposal of structural end-of-life criteria for lifetime prediction.

He is a member of the Executive Board of Polymer Degradation Discussion Group (a subgroup of RSC Macro Group, U.K.) and the Editorial Boards of *Polymer Degradation and Stability* (edited by Elsevier), *Journal of Composites Science* (edited by MDPI), and *Matériaux & Techniques* (edited by EDP Sciences).

• • •